

The Development of a Parameter to Assess Potential for Training Thunderstorms

David Stang

Introduction

Flash flooding is one of the deadliest weather-related hazard in the United States, claiming an average of 87 lives per year from 1989-2018 (NOAA 2018). Flash flooding is most often caused by heavy rainfall, leading to rapidly rising water that can sweep away motor vehicles, and, in more extreme cases, can result in significant property damage and destruction of infrastructure (NOAA). One such mechanism for generating heavy rainfall is “training thunderstorms”, which can be thought of as a line of individual thunderstorms all tracking across the same areas, leading to significant rainfall totals (Figure 1).

Having a parameter to evaluate the potential for training thunderstorms could greatly assist forecasters in assessing the potential severity of a flash flood threat. The development of such a parameter could allow forecasters to more accurately determine when environmental conditions are favorable for training thunderstorms and when environmental conditions are unfavorable for training thunderstorms. This project will also improve my ability to parameterize certain hazards, which will be a skill fundamentally required for my master’s thesis.

Methodology

Maddox 1979 studied synoptic-scale environments in which training thunderstorms were observed. This study found the following characteristics that were largely conducive for training thunderstorms: Quasi-stationary fronts, fast-moving storms whose track was roughly parallel with the front, mean tropospheric wind speeds on the order of 40 kt, and small variations in the wind direction with altitude.

Schwartz et. al. 1990 also noted the observed behavior of the thunderstorm cold pools (currents of cold air produced by thunderstorms). During flash flooding events caused by training thunderstorms, cold pools are largely forced parallel or slightly toward the surface frontal boundary. Strong low-level convergence along the front was also listed as a contributor towards training thunderstorms, leading to continuous redevelopment of new thunderstorms.

Rogash et. al. 2000 highlighted the importance of having strong divergence aloft, leading to strong vertical motions that would contribute to widespread thunderstorm development. The ideal scenario for widespread thunderstorms would be strong divergence aloft co-located with strong convergence near the surface.

Another scenario of training thunderstorms was the potential for training supercell thunderstorms, which tend to track in a slightly different direction than “ordinary” single cells. Bunkers et. al. 2000 developed a method of predicting the motion of (right-moving) supercell thunderstorms given information on the background winds. If supercell thunderstorms are expected on an active weather day, it would be most sensible to consider the Bunkers right motion to predict storm motions instead of the mean wind vector emphasized by Maddox 1979.

In comparison to single cell thunderstorms, flash flooding caused by supercell thunderstorms is rare. Supercell induced flash flooding events are most likely to be caused by slow-moving isolated storms (Bluestein et. al. 2015 and Bunkers et. al. 2016), but a few rare instances of training supercell thunderstorms have been documented (e.g. May 31st, 2013 in El Reno, Oklahoma). Flash flood events that involve training supercell thunderstorms tend to be

catastrophic and lead to extremely high precipitation rates. The El Reno case specifically saw 6”+ rain totals over the course of 2-3 hours (National Weather Service 2013).

Numerical values provided by the aforementioned studies were used to derive a parameter for assessing training thunderstorm potential, which will henceforth be referred to as the Training Axis Parameter (TAP). The first factor considered is a ratio of the mean wind aloft to the forward motion of the front (see Figure 4 for the convention used in the calculation). A combination of strong flow aloft and minimal motion of a frontal boundary would be a contributor to organized training thunderstorms. Weak flow aloft would allow the cold pool to advance thunderstorms away from the front, while a fast-moving front will tend to undercut the thunderstorms that do form and limit their longevity (Figures 2 and 3).

A second factor included was the square root of the mean square deviation of the wind direction with height, given by the below equation:

$$\sigma = \left(\frac{1}{N} \sum_{i=1}^N (\theta_i - \bar{\theta})^2 \right)^{0.5} \quad (1)$$

Where θ_i contains all the wind direction measurements made from the surface up to 100mb or the maximum height of the sounding, whichever has the lowest altitude. Using the values of wind direction provided by Maddox 1979, the square root of the mean square deviation comes out to be approximately 25°. Lower values of σ imply an atmosphere that has a more organized and unidirectional wind profile, thereby tending to favor single cell (or even multi-cell) thunderstorms organizing into a “training axis”.

A third factor included in the calculation was the angle between the expected storm direction and the velocity vector of the front (Figure 4). For “ordinary” thunderstorms, this is simply taken as the mean wind vector, and the angle is represented as α . For supercell thunderstorms, the angle is between the Bunkers right motion vector, and this angle is represented as β . Also, for supercells, the σ variable was excluded since supercell environments typically have strong veering winds, which would yield large values for σ . Another difference is the supercell variation also includes a ratio of Most-Unstable Convective Available Potential Energy (MUCAPE) to Lifted Condensation Level (LCL) in accordance with the findings of Bunkers et. al. 2016.

The combination of surface convergence and upper air divergence was also included in the original version of the TAP, however, obtaining consistent historical data on these parameters (for the purposes of verifying the TAP’s accuracy) proved to be a challenge, thus it was excluded.

Combining all of these factors gives:

$$\text{TAP (Ordinary)} = \left(\frac{|\mathbf{v}|}{|\mathbf{v}_F| + \gamma_v} \right) \left(\frac{2\gamma^\theta}{\sigma + \gamma^\theta} \right) \sin^2\alpha \quad (2a)$$

$$\text{TAP (Supercell)} = \left(\frac{|\mathbf{v}_{rm}|}{|\mathbf{v}_F| + \gamma_v} \right) \left(\frac{MUCAPE}{LCL + \gamma_{LCL}} \right) \sin^2\beta \quad (2b)$$

Where \mathbf{v} is the mean wind vector, \mathbf{v}_F is the forward motion vector of the front, \mathbf{v}_{RM} is the Bunkers right vector, σ is the quantity obtained from equation (1), α is the angle between \mathbf{v} and \mathbf{v}_F , and β is the angle between \mathbf{v}_F and \mathbf{v}_{RM} . The factors of γ that appear are used to “soften” the inverse proportionality, i.e. prevent very small values from “blowing up” the value of the parameter. The values for γ were determined by using values provided in the literature and ensuring that, when those values are applied to the TAP equations, the respective terms come out to be 1. Approximating 8 kt as a favorable value for \mathbf{v}_F and using 40 kt as a favorable value for \mathbf{v} and \mathbf{v}_{RM} , γ_v comes out to be approximately 30 kt. Using 25° as a favorable value for σ , γ^θ comes out to be approximately 25° . In the case of the angle α , an ideal environmental for training thunderstorms would have \mathbf{v}_F and \mathbf{v} being orthogonal (perpendicular, $\pm 90^\circ$) to each other, which would thereby maximize the value of $\sin^2\alpha$ (and $\sin^2\beta$ in the case of \mathbf{v}_{RM} and \mathbf{v}_F). For the MUCAPE/LCL ratio, the upper bound of 2000 J/kg provided by Bunkers et. al. 2016 was used in conjunction with an LCL of 1000 meters, which would make γ_{LCL} be $1000 \text{ m}^{-1} \text{ J}^{-1} \text{ kg}$.

To verify the accuracy of the parameter, observed sounding data for past flooding events was obtained near the location of the most significant flooding. Regional surface observations were used to approximate the orientation (to the nearest 15°) and movement of the front (to the nearest 5 kt) responsible for triggering the convection. This proved to be a significant challenge since a complete archive of all North American flash flood events could not be found. As a result, the Weather Prediction Center’s (WPC) past Excessive Rainfall Outlooks (EROs) were used to determine what dates had an appreciable flooding risk. Most of the past events analyzed were moderate and high risk days, but some of the events from the aforementioned literature were also analyzed. Please refer to Table 1 to see a complete list of the events analyzed and the sounding that was used.

Results and Discussion

Of the events examined (see Table 1 for a complete list) that involved ordinary thunderstorms (not supercells), 84% of the cases had a TAP value of at least 0.5 with somewhat of a normal distribution evident in Figure 5. This would suggest that TAP values greater than 0.5 can be associated with environments favorable for training non-supercell thunderstorms.

The highest value calculated from the cases examined was 1.61 for a high-impact flash flooding event that occurred on May 22, 2019 where significant flooding rains were observed in and near Tulsa, Oklahoma. Up to 11” of rain was observed over the course of 3 days in this region (National Weather Service 2019). However, in the years spanning from 2015 to 2019, arguably the most textbook setup for training thunderstorms occurred in March of 2016 over portions of Louisiana and Arkansas where up to 20” of rain fell over the course of 3-4 days (National Weather Service 2016). The TAP value for this event (based on the 3/10/2016 12Z Shreveport, LA sounding) came out to be 1.07. However, on this Shreveport sounding, there was a wind shift evident in the lowest 1 km associated with a frontal passage, which resulted in an errantly high value for σ . When this data was removed, the TAP value came out to be 2.11, which is easily the highest TAP value in the dataset for ordinary thunderstorms.

As already mentioned, setups that favor training supercell thunderstorms are rare in comparison to setups that favor training ordinary thunderstorms. As a result, very few cases were able to be studied. However, the cases mentioned in Rogash et. al. 2000, Bluestein et. al. 2015, and Bunkers et. al. 2016 were tested against the TAP equation for supercells. Three other cases which observed training supercells since these publications were on March 28, 2017; May 22, 2019; and April 13, 2019. Based on the data shown in Table 1, supercell TAP values above 1 appear to be favorable for training supercells. The values well below 1 were more associated with slow-moving supercells as opposed to supercells that tracked along a frontal boundary.

Conclusion

The main goal of this project was to use past literature to devise a parameter that would identify environments favorable for training convection capable of causing flash flooding. Based on the results of the verification, at least some success has been achieved. However, there is still room for additional analysis and room for additional improvement. For one, there was an element of subjectivity used in evaluating the parameter, namely the orientation and motion of synoptic scale fronts. The original plan was to use an algorithm to objectively (and more accurately) determine this information, but there was not enough time or computational power at hand to apply this algorithm.

Another important caveat to note is that the TAP parameter has not been extensively tested against cases where training thunderstorms did not occur. Without this information, it is impossible to gauge what false alarm rate might result from using the TAP as a forecasting tool. However, it can be said that the TAP is at least somewhat capable of identifying environments favorable for training thunderstorms, which is a crucial step in the right direction.

Overall, the primary goal of this project was accomplished, and this skill of combining previous findings and observations into a parameter has been well-developed. The secondary goal (whether or not it improves the forecasting process) has yet to be evaluated. Testing the parameter on model output and then determining probabilities of detection and false alarm rates would probably be the best way to accomplish this secondary goal.

There was also an important factor of convergence and divergence that was omitted, because archived datasets containing this information could not be found in the time allotted. Another possible course of future work would be to put a convergence/divergence term into the parameter and then reanalyze past flash flooding events caused by training thunderstorms.

A few other factors could potentially be included in the parameter to improve performance. For one, the parameter currently does not account for katafrontal or anafrontal boundaries. Anafrontal boundaries would be most favorable for flooding since these boundaries allow for precipitation to continue over the stable side of the boundary. Furthermore, this version of the parameter was primarily concerned with the dynamics that favor training convection. Factoring in thermodynamic variables (particularly moisture variables) should also improve the parameter's performance. Finally, implementing an algorithm that would more precisely determine numerical values for the angle of the surface front and the forward motion vector of the surface front would also improve the evaluation process.

References

Bluestein, H. B., J. C. Snyder, J. B. Houser, 2015: A Multiscale Overview of the El Reno, Oklahoma, Tornadoic Supercell of 31 May 2013. *Bull. Amer. Meteor. Soc.*, **30**, 525-552, <https://journals.ametsoc.org/doi/pdf/10.1175/WAF-D-14-00152.1>

Bunkers, M. J., C. A. Doswell III, 2016: Comments on “Double Impact: When Both Tornadoes and Flash Floods Threaten the Same Place at the Same Time”. *Bull. Amer. Meteor. Soc.*, **31**, 1715-1721, <https://journals.ametsoc.org/doi/pdf/10.1175/WAF-D-16-0116.1>

Bunkers, M. J., B. A. Klimowski, J. W. Zeitler, R. L. Thompson, M. L. Weisman, 2000: Predicting Supercell Motion Using a New Hodograph Technique. *Bull. Amer. Meteor. Soc.*, **15**, 61-79, <https://w2.weather.gov/media/unr/soo/scm/BKZTW00.pdf>

Maddox, R. A., 1970: A methodology for forecasting heavy convective precipitation and flash flooding. *National Weather Digest*, <http://citeserx.ist.psu.edu/viewdoc/download?doi=10.1.1.663.8634&rep=rep1&type=pdf>

National Weather Service, 2019: 20-22 May 2019 Tornado and Flooding Event. Accessed 21 November 2019, https://www.weather.gov/sgf/20_22May2019_TornadoHydro

National Weather Service, 2013: Flooding and Rainfall Information Related to the May 31-June 1, 2013 Tornado and Flash Flood Event. Accessed 20 November 2019, <https://www.weather.gov/oun/events-20130531-flooding>

National Weather Service, 2016: March 8-11, 2016: Heavy Rain and Flooding. Accessed 19 November 2019, https://www.weather.gov/shv/event_2016-03-09_flooding

NOAA, 2018: Weather Related Fatality and Injury Statistics. Accessed 18 November 2019, <https://www.weather.gov/hazstat/>

NOAA: Flood Related Hazards. Accessed 22 November 2019, <https://www.weather.gov/safety/flood-hazards>

Rogash, J. A., R. D. Smith, 2000: Multiscale Overview of a Violent Tornado Outbreak with Attendant Flash Flooding. *Bull. Amer. Meteor. Soc.*, **15**, 416-431, <https://journals.ametsoc.org/doi/pdf/10.1175/1520-0434%282000%29015%3C0416%3AMOOAVT%3E2.0.CO%3B2>

Schwartz, B. E., C. F. Chappell, W. E. Togstad, X. P. Zhong, 1990: The Minneapolis Flash Flood: Meteorological Analysis and Operational Response. *Bull. Amer. Meteor. Soc.*, **5**, 3-20, <https://journals.ametsoc.org/doi/pdf/10.1175/1520-0434%281990%29005%3C0003%3ATMFFMA%3E2.0.CO%3B2>

Weather Prediction Center: WPC's Excessive Rainfall Outlook Archive. Accessed 11 November 2019, https://www.wpc.ncep.noaa.gov/archives/web_pages/ero/ero.shtml

Figures and Tables

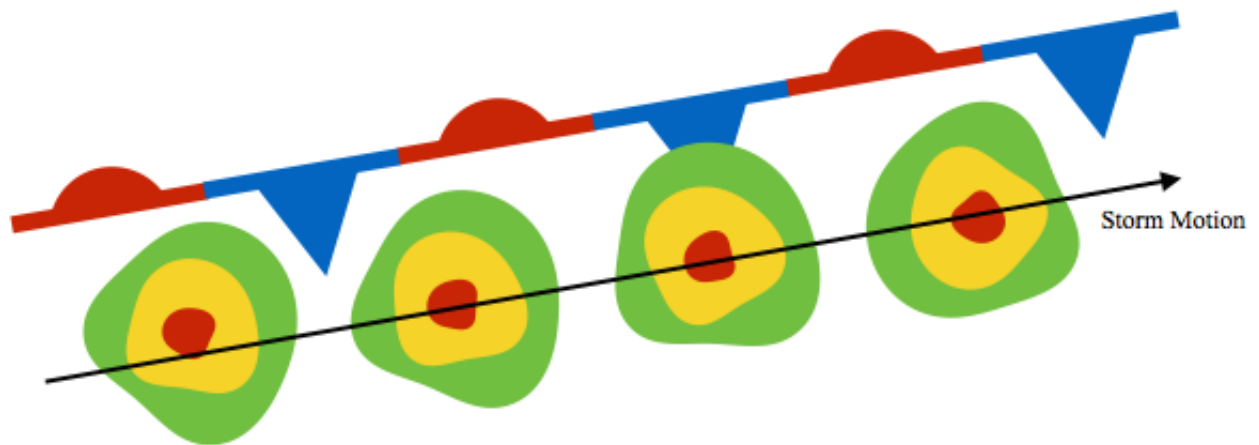


Figure 1. This figure shows a conceptual diagram of “training thunderstorms”. Each individual storm tracks over the same area, resulting in heavy rainfall and flash flooding.

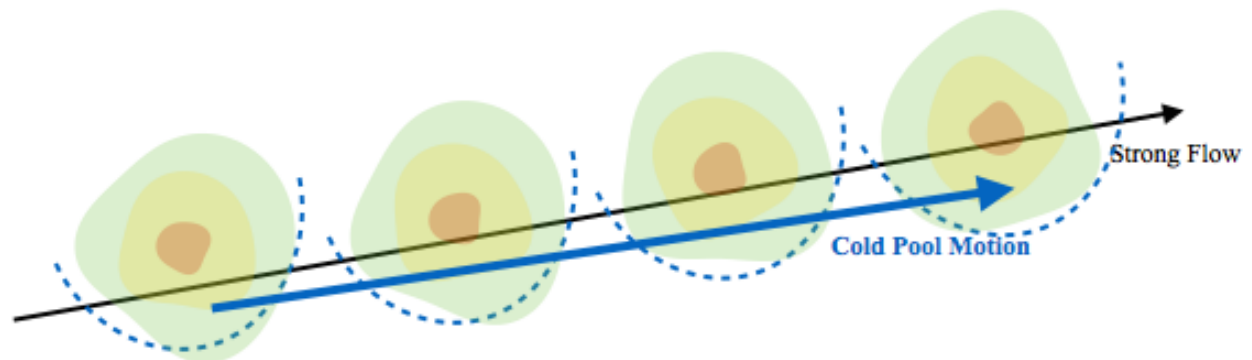


Figure 2. This figure shows the behavior of thunderstorm cold pools in the presence of strong flow aloft. When strong flow is present, cold pools are forced away from the thunderstorm updrafts, allowing the individual storms to stay aligned with the front.

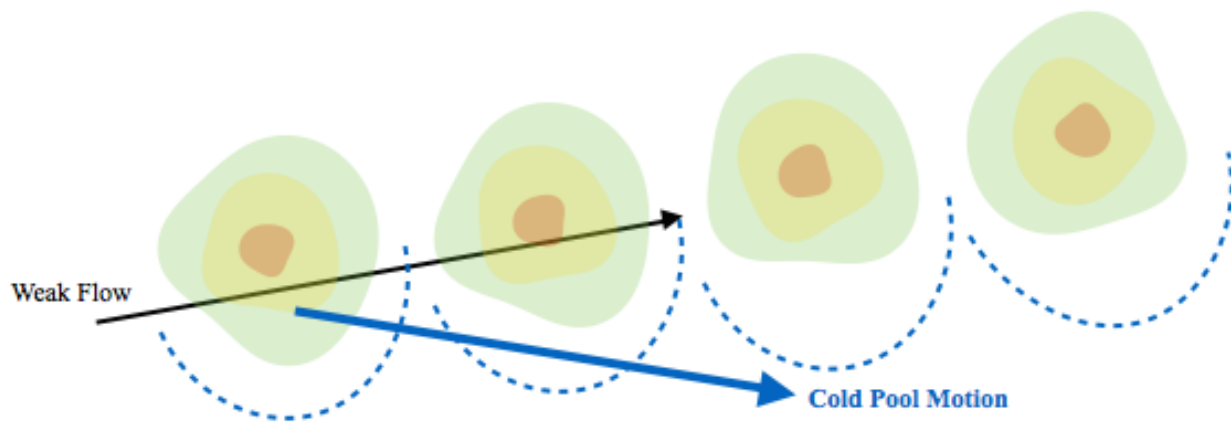


Figure 3. This figure shows the behavior of thunderstorm cold pools in the presence of weak flow aloft. When weak flow is present, cold pools are allowed to undercut thunderstorm updrafts, which ultimately limits updraft longevity and limits the potential for organized training.

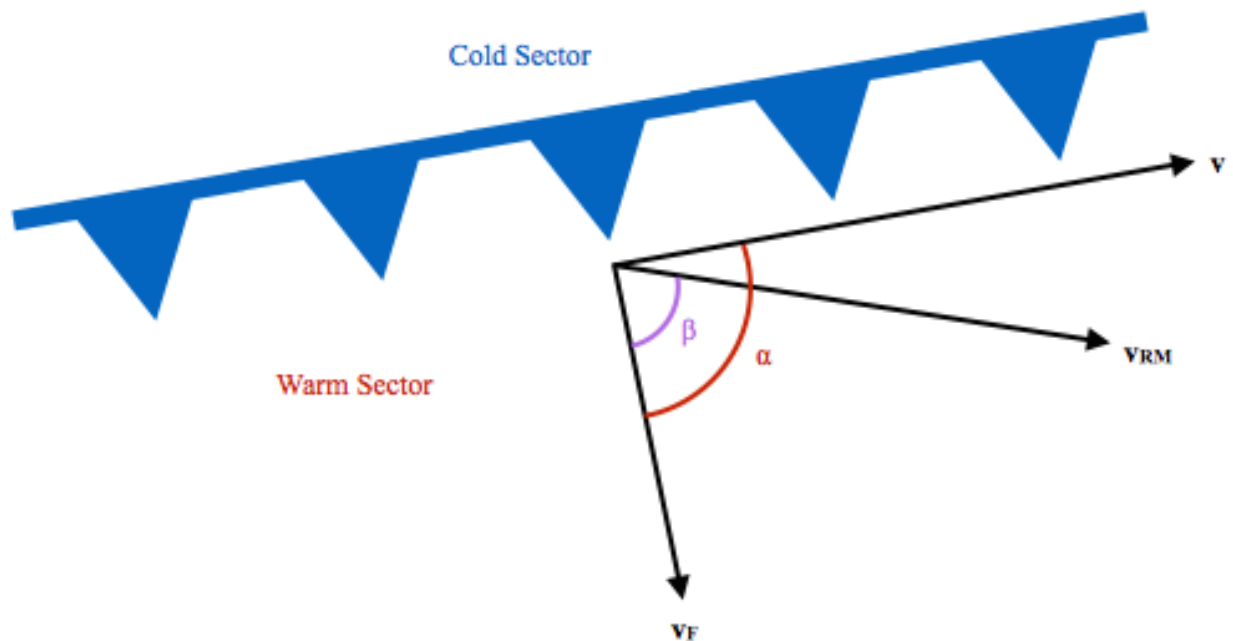


Figure 4. This figure shows the vectors used in the training axis parameter calculation. v_F represents the forward motion of the frontal boundary, v represents the mean flow, and v_{RM} is the Bunkers right motion vector. Additionally, α is the angle between v_F and v , while the β is the angle between v_{RM} and v_F .

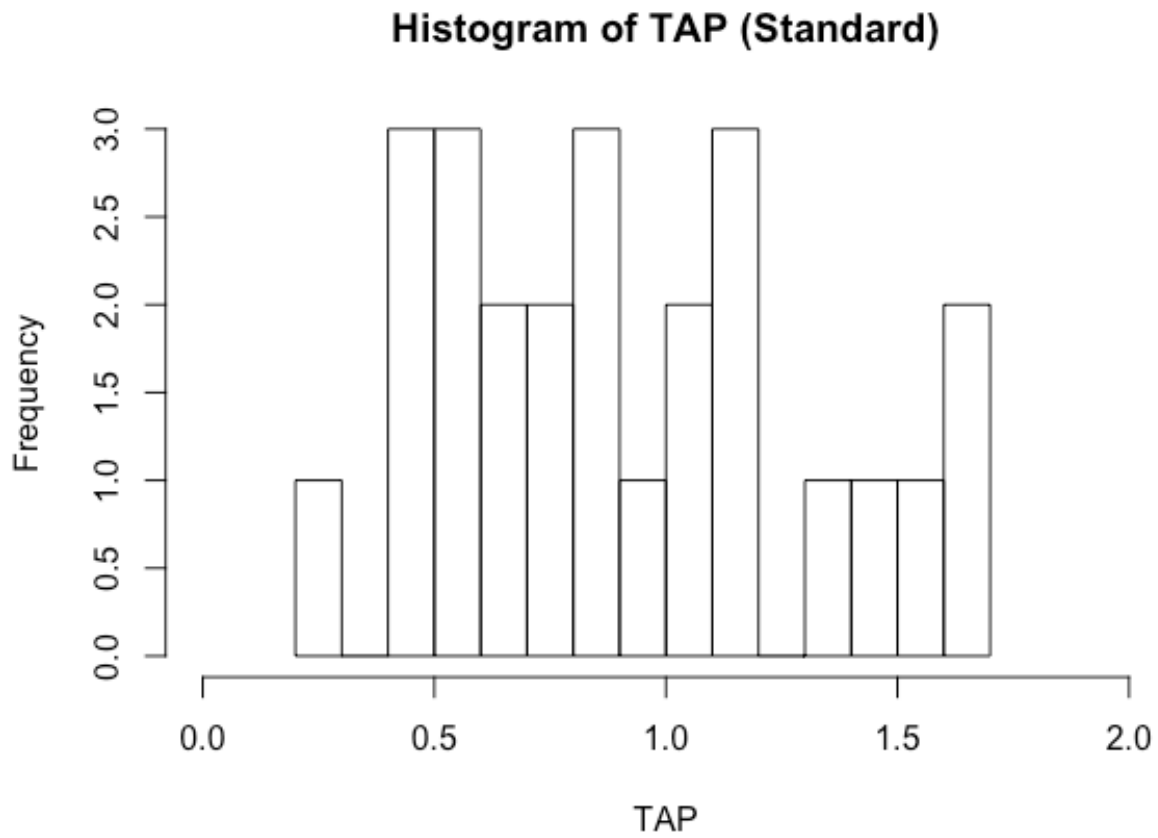


Figure 5. This figure shows a histogram (distribution) of the Training Axis Parameter (TAP) values calculated for each case examined that involved ordinary thunderstorms (not supercells).

Table 1. This table shows the cases used to evaluate the accuracy of the TAP parameter.

SOUNDING	TAP	WPC RISK	TYPE
05-24-2015 00Z FWD	0.741	Unknown	Ordinary
05-29-2015 00Z FWD	0.470	Unknown	Ordinary
03-10-2016 12Z SHV	1.070	High	Ordinary
03-25-2017 00Z LZK	1.610	Slight	Ordinary
03-31-2017 00Z BNA	1.423	Slight	Ordinary
04-16-2017 00Z DDC	0.718	Marginal	Ordinary
04-21-2017 00Z OUN	0.502	Slight	Ordinary
04-29-2017 00Z OUN	0.609	Moderate	Ordinary
04-29-2017 18Z LZK	0.849	High	Ordinary
04-30-2017 12Z JAN	1.155	Moderate	Ordinary
05-03-2017 18Z LIX	0.258	Moderate	Ordinary
05-20-2017 00Z FWD	0.889	Moderate	Ordinary
05-23-2017 00Z LIX	0.447	Moderate	Ordinary
04-14-2018 00Z LZK	1.139	Moderate	Ordinary
04-14-2018 12Z JAN	1.597	Moderate	Ordinary
11-01-2018 00Z LZK	0.623	Slight	Ordinary
05-10-2019 12Z LCH	0.578	High	Ordinary
05-23-2019 00Z SGF	1.610	Moderate	Ordinary
05-25-2019 00Z SGF	0.916	High	Ordinary
05-26-2019 00Z TOP	1.175	Moderate	Ordinary
05-27-2019 00Z DDC	1.349	Moderate	Ordinary
05-29-2019 12Z FWD	1.093	Moderate	Ordinary
04-04-2019 12Z LIX	0.403	Moderate	Ordinary
04-06-2019 12Z FWD	0.528	Slight	Ordinary
04-07-2019 12Z SHV	0.819	Slight	Ordinary
05-31-2013 18Z OUN	1.780	Unknown	Supercell
03-02-1997 00Z LZK	1.443	Unknown	Supercell
06-23-2003 00Z TOP	0.029	Unknown	Supercell
11-16-2001 00Z CRP	0.046	Unknown	Supercell
03-29-2017 00Z OUN	0.418	Slight	Supercell
05-23-2019 00Z SGF	2.569	Moderate	Supercell
04-13-2019 18Z JAN	0.454	Moderate	Supercell